

CERN-EP-2021-230
03 November 2021

Measurement of the photon polarization in $\Lambda_b^0 \rightarrow \Lambda \gamma$ decays

LHCb collaboration[†]

Abstract

The photon polarization in $b \rightarrow s \gamma$ transitions is measured for the first time in radiative b -baryon decays exploiting the unique spin structure of $\Lambda_b^0 \rightarrow \Lambda \gamma$ decays. A data sample corresponding to an integrated luminosity of 6 fb^{-1} collected by the LHCb experiment in pp collisions at a center-of-mass energy of 13 TeV is used. The photon polarization is measured to be $\alpha_\gamma = 0.82^{+0.17+0.04}_{-0.26-0.13}$, where the first uncertainty is statistical and the second systematic. This result is in agreement with the Standard Model prediction and previous measurements in b -meson decays. Charge-parity breaking effects are studied for the first time in this observable and found to be consistent with CP symmetry.

Submitted to Phys. Rev. Lett.

© 2021 CERN for the benefit of the LHCb collaboration. CC BY 4.0 licence.

[†]Authors are listed at the end of this paper.

Rare decays of hadrons containing b -quarks mediated by flavor-changing neutral currents (FCNC) are suppressed in the Standard Model (SM) since they occur only at higher order in the perturbative expansion. They are sensitive to physics beyond the SM (BSM) which can give additional contributions and alter the decay properties. Radiative decays of the type $b \rightarrow s\gamma$ are FCNC, mediated by electroweak-loop transitions which produce a final state photon. In the SM, due to the chirality of the electroweak interaction, the emitted photons are polarized. The photon polarization is defined as the normalized difference between the number of left-handed (γ_L) and right-handed (γ_R) photons produced in radiative decays,

$$\alpha_\gamma \equiv \frac{\gamma_L - \gamma_R}{\gamma_L + \gamma_R}, \quad (1)$$

with photons emitted in b decays being predominantly left-handed. Right-handed contributions arise only due to chirality flips in the outgoing s -quark line of the Feynman diagram, which are suppressed by the ratio of the s and b quark masses. At leading order in the SM, the photon polarization is predicted to be $\alpha_\gamma = (1 - |r|^2)/(1 + |r|^2)$, with $|r| \approx m_s/m_b$ [1–3]. Effects arising at next-to-leading order are estimated to be at the percent level [2]. Therefore, a larger right-handed polarization, which would lower the value of α_γ , could be a clear indication of BSM physics [1, 4].

The photon polarization in $b \rightarrow s\gamma$ transitions has been indirectly probed by the BaBar, Belle and LHCb experiments through the measurement of mixing-induced charge-parity (CP) asymmetries in B^0 and B_s^0 decays [5–7] and through the angular analysis of $B^0 \rightarrow K^{*0}e^+e^-$ decays at very low dielectron mass [8], with the latter providing the strongest constraints on right-handed currents. Radiative decays of b baryons offer a unique opportunity for a direct measurement of the photon polarization due to the nonzero spin of the initial- and final-state particles [9]. The $\Lambda_b^0 \rightarrow \Lambda\gamma$ decay¹ is of special interest due to the weak decay of the Λ baryon, which probes the helicity structure of the $b \rightarrow s\gamma$ transition through the measurement of the Λ helicity [2, 10]. The $\Lambda_b^0 \rightarrow \Lambda\gamma$ decay was first observed in data recorded by LHCb during 2016 [11]. The photon-polarization sensitivity using this decay was estimated in Ref. [12].

The angular distribution of $\Lambda_b^0 \rightarrow \Lambda\gamma$ decays, where the Λ baryon decays into a proton and a pion, is given by the differential width [3]

$$\frac{d\Gamma}{d(\cos\theta_p)} \propto 1 - \alpha_\gamma\alpha_\Lambda \cos\theta_p, \quad (2)$$

where α_Λ is the Λ weak decay parameter and θ_p is the angle between the proton momentum in the Λ rest frame and the Λ momentum in the Λ_b^0 rest frame. The photon direction is integrated over in this study since the distribution in this variable is flat for unpolarized Λ_b^0 baryons, as produced at the LHC [13, 14].

Contrary to b decays, photons produced in \bar{b} decays are expected to be predominantly right-handed in the SM, resulting in a photon polarization of $\alpha_\gamma = -1$. A discrepancy in the absolute value of the photon polarisation in b and \bar{b} decays would be a hint of CP asymmetry in these transitions. In the SM, CP asymmetries in $b \rightarrow s\gamma$ decays are estimated to be less than $\mathcal{O}(1\%)$ [2]. However, new CP -violating BSM contributions can produce asymmetries of $\mathcal{O}(10\%)$ [2]. Experimentally, the strongest constraint on direct

¹The inclusion of charge-conjugate processes is implied throughout, except in the discussion of asymmetries.

CP violation in $b \rightarrow s\gamma$ transitions is from $B^0 \rightarrow K^{*0}\gamma$ decays [15]. Measurements of angular asymmetries and CP -conjugated decay branching ratios can separate the CP -odd and CP -even components of both the SM and opposite chirality contributions to the $\Lambda_b^0 \rightarrow \Lambda\gamma$ decay rate [2].

This Letter reports the first measurement of the photon polarization in $\Lambda_b^0 \rightarrow \Lambda\gamma$ decays, with $\Lambda \rightarrow p\pi^-$, using a data sample corresponding to an integrated luminosity of 6 fb^{-1} collected by the LHCb experiment in proton-proton (pp) collisions at a center-of-mass energy of 13 TeV during 2015–2018. Additionally, the first study of CP angular asymmetries in $b \rightarrow s\gamma$ decays is performed.

The LHCb detector [16, 17] is a single-arm forward spectrometer covering the pseudorapidity range $2 < \eta < 5$, designed for the study of particles containing b or c quarks. The detector elements that are relevant for this analysis are: a silicon-strip vertex detector surrounding the pp interaction region that allows c and b hadrons to be identified from their characteristically long flight distance; a tracking system that provides a measurement of the momentum of charged particles; two ring-imaging Cherenkov detectors that are able to discriminate between different species of charged hadrons; a calorimeter system consisting of scintillating-pad and preshower detectors, an electromagnetic calorimeter (ECAL) and a hadronic calorimeter, that enables the reconstruction and identification of photons, electrons and hadrons; and a muon system composed of alternating layers of iron and multiwire proportional chambers.

Charged and neutral clusters in the ECAL are separated by extrapolating reconstructed tracks to the ECAL; photons and neutral pions are distinguished by their cluster shape and energy distribution. For decays with high-energy photons in the final state, *e.g.* $\Lambda_b^0 \rightarrow \Lambda\gamma$, a mass resolution around 100 MeV is achieved² [18, 19], dominated by the photon energy resolution. The online event selection is performed by a trigger [20], consisting of a hardware stage followed by a software stage which fully reconstructs the event. The hardware trigger requires events to have an ECAL cluster with an energy component transverse to the beam, E_T , above a threshold varying between 2.1 – 3.0 GeV. The software trigger first requires at least one charged particle to have transverse momentum $p_T > 1$ GeV and to be inconsistent with originating from any primary pp collision vertex (PV). Subsequently, Λ candidates are formed from two tracks significantly displaced from any PV, and combined with a high- E_T photon to identify decays consistent with the signal mode. In the offline selection, trigger signals are associated with reconstructed particles and only events where the trigger was activated by the decay products of the signal candidate are kept.

Simulated events are used to model the effects of the detector geometry and the selection requirements. In the simulation, pp collisions are generated using PYTHIA [21] with a specific LHCb configuration [22]. Decays of unstable particles are described by EVTGEN [23], in which final-state radiation is generated using PHOTOS [24]. The interaction of the generated particles with the detector, and its response, are implemented using the GEANT4 toolkit [25] as described in Ref. [26]. The signal sample is generated with unpolarized Λ_b^0 decays and only a left-handed photon contribution. The simulation is validated using the $\Lambda_b^0 \rightarrow pK^- J/\psi$ and $\Lambda_b^0 \rightarrow \Lambda J/\psi$, with $J/\psi \rightarrow \mu^+\mu^-$, control modes in data. The $\Lambda_b^0 \rightarrow pK^- J/\psi$ mode is selected according to Ref. [27], while the $\Lambda_b^0 \rightarrow \Lambda J/\psi$ mode is selected with the strategy described for the signal mode below. The Λ_b^0

²Natural units with $\hbar = c = 1$ are used throughout.

momentum distribution of all simulated samples with Λ_b^0 decays is corrected to data in two-dimensional intervals of Λ_b^0 transverse momentum and pseudorapidity, $p_T(\Lambda_b^0)$ and $\eta(\Lambda_b^0)$, using $\Lambda_b^0 \rightarrow pK^- J/\psi$ background-subtracted data and simulated candidates.

Offline signal candidates are reconstructed from the combination of a Λ baryon and a high-energy photon candidate. Opposite-charge good-quality track pairs, well separated from any PV, are combined to form Λ candidates, where one track is consistent with the proton hypothesis and the other with the pion hypothesis. Proton and pion candidates are required to have p_T larger than 800 MeV and 300 MeV, respectively. The Λ candidate must form a good-quality vertex that is well separated from the nearest PV and have a mass in the range 1110–1122 MeV. Only Λ candidates that decay in the central part of the vertex detector ($z < 270$ mm) and have a p_T larger than 1 GeV are retained for further study. Photons, reconstructed from clusters in the ECAL, must have $E_T > 3$ GeV and be inconsistent with the extrapolation of reconstructed tracks to the ECAL. Since the Λ_b^0 decay vertex cannot be reconstructed in this mode, the photon is assumed to originate from the pp interaction region. The sum of the Λ p_T and the photon E_T must be larger than 5 GeV. The Λ_b^0 candidate must have a transverse momentum above 4 GeV and a mass within 900 MeV of the known Λ_b^0 mass [28]. The distance of closest approach between the Λ_b^0 and Λ trajectories is required to be small; the Λ_b^0 trajectory is assumed to originate from the PV closest to the Λ trajectory

A boosted decision tree (BDT) [29], implementing the XGBoost algorithm [30], used within the Scikit-learn library [31], separates signal from combinatorial background, which is formed by combinations of a real Λ baryon with a random photon. The BDT classifier is trained on a signal sample of $\Lambda_b^0 \rightarrow \Lambda\gamma$ simulated events and a background sample from data candidates with a mass larger than 6.1 GeV. The same variables of Ref. [11], with the addition of the photon pseudorapidity, are used as input for the classifier. To maximize sensitivity to the photon polarization, the BDT threshold is selected to reject 99% of background and retain around 50% of signal candidates.

The mass distribution of the selected candidates is shown in Fig. 1. A fit to this mass distribution is used to determine the signal and background yields. The $\Lambda_b^0 \rightarrow \Lambda\gamma$ signal component is modeled with a Crystal Ball [32] probability density function (PDF), with power-law tails above and below the Λ_b^0 mass. The tail parameters and the width of the signal peak are fixed to values determined from simulation while the mean is allowed to vary freely in the fit to data. A comprehensive set of background contributions is investigated but only two are found to be significant [11]. The dominant contribution is from combinatorial background which is modeled by an exponential PDF with a freely varying slope. A small contamination from $\Lambda_b^0 \rightarrow \Lambda\eta$ decays with $\eta \rightarrow \gamma\gamma$, where one of the photons is not reconstructed, is also expected and is described with the shape determined from simulation. The signal and combinatorial background yields vary freely in the fit to data, while the yield of $\Lambda_b^0 \rightarrow \Lambda\eta$ is constrained to its expected value, obtained from its measured branching fraction [28] and reconstruction and selection efficiencies determined from simulation.

The signal and background yields are obtained from an extended unbinned maximum likelihood fit to data, as shown in Fig. 1 (left). In the signal region, [5387.1, 5852.1] MeV, the signal yield is 440 ± 40 , with 1460 ± 23 and 10 ± 4 combinatorial and $\Lambda_b^0 \rightarrow \Lambda\eta$ decays, respectively.

The photon polarization is measured with an unbinned maximum likelihood fit to the $\cos\theta_p$ distribution for events in the signal region, as shown in Fig. 1 (right). The signal is

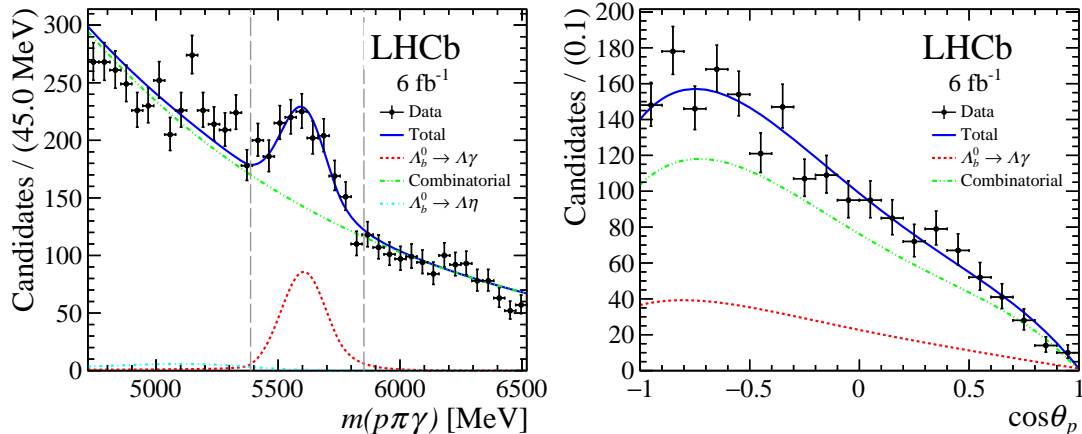


Figure 1: Distribution of (left) mass, $m(p\pi\gamma)$, and (right) $\cos\theta_p$ for $\Lambda_b^0 \rightarrow \Lambda\gamma$ candidates. The latter shows the subset of candidates in the signal region $m(p\pi\gamma) \in [5387.1, 5852.1]$ MeV, delimited by dashed vertical lines in the former. The results of the fits are overlaid as well as the individual contributions.

described by the PDF in Eq. (2) multiplied by an acceptance function, which accounts for the effect of the detector geometry, reconstruction and selection requirements. The photon polarization parameter, α_γ , is allowed to vary freely in the fit to data, whereas the physical boundary $[-1, 1]$ on this parameter is imposed later using the Feldman-Cousins technique [33]. The Λ weak decay parameter, α_Λ , is fixed to the average of the values measured by BESIII in Λ and $\bar{\Lambda}$ decays, $\alpha_\Lambda = 0.754 \pm 0.004$ [34]. The shape of the acceptance in $\cos\theta_p$ is determined from simulation and is parametrized as a fourth order polynomial. It is dominated by the impact parameter and transverse momentum requirements on the proton and the pion. The correct description of the acceptance in simulation is validated using $\Lambda_b^0 \rightarrow \Lambda J/\psi$ decays, which are reconstructed without using information from the J/ψ vertex. This decay mode, with higher yield and purity than that of the signal mode, has the same final-state hadrons. The combinatorial and $\Lambda_b^0 \rightarrow \Lambda\eta$ components are described together by a fourth-order polynomial, with the coefficients determined from a fit to the candidates in the Λ_b^0 mass control region $[4719.6, 5382.1] \cup [5857.1, 6519.6]$ MeV. The values of these coefficients are found to be consistent for candidates below and above the signal region. The ratio between signal and background decays is constrained by the yields obtained from the mass fit. The fit stability is validated with pseudoexperiments and the results were only examined after all analysis procedures had been finalized in order to avoid experimenter's bias. The result of the fit to data candidates is $\alpha_\gamma = 0.82 \pm 0.23$, where the uncertainty is obtained from the Hessian matrix.

The data are separated into $\Lambda_b^0 \rightarrow \Lambda\gamma$ and $\bar{\Lambda}_b^0 \rightarrow \bar{\Lambda}\gamma$ by the charge of the final-state pion and potential CP breaking effects on the photon polarization are studied. The photon polarization values in $\Lambda_b^0 \rightarrow \Lambda\gamma$ and $\bar{\Lambda}_b^0 \rightarrow \bar{\Lambda}\gamma$ decays, denoted as α_γ^- and α_γ^+ , are expected to have the same absolute value with opposite sign in the absence of CP violation. Both values are measured independently for Λ_b^0 and $\bar{\Lambda}_b^0$ decays following the same strategy as described for the combined sample. The shape of the mass distribution for Λ_b^0 and $\bar{\Lambda}_b^0$ decays is studied in simulation and is compatible, for both signal and $\Lambda_b^0 \rightarrow \Lambda\eta$ decays, therefore the shape from the combined sample is used in the fit of the two data sets. In the

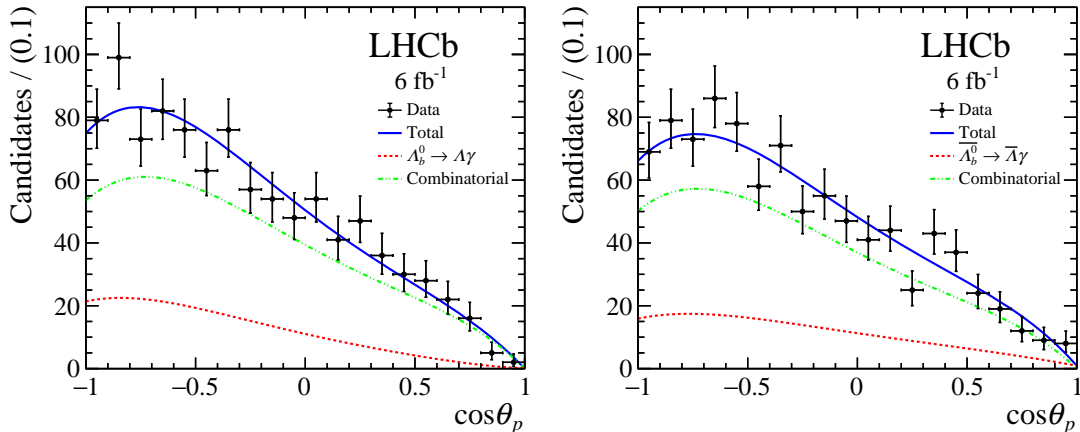


Figure 2: Distribution of $\cos\theta_p$ for selected (left) $\Lambda_b^0 \rightarrow \Lambda\gamma$ and (right) $\bar{\Lambda}_b^0 \rightarrow \bar{\Lambda}\gamma$ candidates as well as the individual contributions.

signal region, 233 ± 32 $\Lambda_b^0 \rightarrow \Lambda\gamma$ and 210 ± 30 $\bar{\Lambda}_b^0 \rightarrow \bar{\Lambda}\gamma$ decays are found. These yields are affected by production and detection asymmetries [35] and cannot be directly interpreted as a measurement of CP -violation effects. The Λ and $\bar{\Lambda}$ weak-decay parameters measured by BESIII [34], $\alpha_{\Lambda}^- = 0.750 \pm 0.009 \pm 0.004$ and $\alpha_{\Lambda}^+ = -0.758 \pm 0.010 \pm 0.007$, are used in the angular fit for $\Lambda_b^0 \rightarrow \Lambda\gamma$ and $\bar{\Lambda}_b^0 \rightarrow \bar{\Lambda}\gamma$, respectively. Due to the limited sample size, the acceptance and background shapes are taken from the combined sample. The fit to data candidates yields $\alpha_{\gamma}^- = 1.26 \pm 0.42$ and $\alpha_{\gamma}^+ = -0.55 \pm 0.32$, where the uncertainty is statistical only. The results of the angular fits are shown in Fig. 2.

Systematic uncertainties associated with the determination of the signal and background yields in the mass fit, the modeling of the background shape and signal acceptance and the finite precision on the external parameter α_{Λ} are evaluated. These uncertainties are determined by fitting pseudosamples, generated by an alternative model, with the default model. The limited data size from the mass control region used to determine the background angular shape dominates this uncertainty and is evaluated by varying the background shape parameters. The systematic uncertainty of the background parameterization is evaluated using a third and fifth degree polynomial. The acceptance uncertainty is evaluated by considering the limited size of the simulation, using alternative fifth and third degree parametrizations, and removing the Λ_b^0 kinematic corrections. The mass fit uncertainty is determined with pseudoexperiments using an alternative model with a variable signal width. Finally, the limited precision of the Λ decay parameter introduces a small systematic uncertainty. The photon polarization, with all systematic uncertainties included, is $\alpha_{\gamma} = 0.82 \pm 0.23 \pm 0.13$.

For the CP asymmetry measurement, the uncertainties described above are 100% correlated and sum to 0.13 and 0.11 for α_{γ}^- and α_{γ}^+ , respectively. Additional uncertainties arise from potential differences in the background shape and signal acceptance between Λ_b^0 and $\bar{\Lambda}_b^0$ decays. Fits are performed with the default combined model to pseudosamples generated with alternative models obtained independently for Λ_b^0 and $\bar{\Lambda}_b^0$ candidates, to estimate this effect. These uncertainties are uncorrelated and are 0.15 and 0.12 for α_{γ}^- and α_{γ}^+ , respectively, resulting in $\alpha_{\gamma}^- = 1.26 \pm 0.42 \pm 0.20$ and $\alpha_{\gamma}^+ = -0.55 \pm 0.32 \pm 0.16$.

Confidence intervals on the photon polarization are set within the physical limits of $[-1, 1]$, see Eq. 1, using the Feldman-Cousins technique, the fit result, and the relation

between the true and measured values obtained from pseudoexperiments, including both statistical and systematic uncertainties. The photon polarization in $\Lambda_b^0 \rightarrow \Lambda \gamma$ decays is found to be

$$\alpha_\gamma = 0.82_{-0.26}^{+0.17} \text{ (stat.) }_{-0.13}^{+0.04} \text{ (syst.)},$$

which is compatible with the SM prediction. This result excludes two regions allowed by previous measurements for the Wilson coefficients of the effective Hamiltonian of the $b \rightarrow s \gamma$ transition (see the Supplemental material to this Letter for details).

The Feldman-Cousins technique is also applied to the photon polarization measurements in $\Lambda_b^0 \rightarrow \Lambda \gamma$ and $\bar{\Lambda}_b^0 \rightarrow \bar{\Lambda} \gamma$ decays, which are found to be

$$\begin{aligned} \alpha_\gamma^- &> 0.56 \text{ (0.44) at 90\% (95\%) CL,} \\ \alpha_\gamma^+ &= -0.56_{-0.33}^{+0.36} \text{ (stat.) }_{-0.09}^{+0.16} \text{ (syst.),} \end{aligned}$$

consistent with CP symmetry.

To summarize, the photon polarization in $b \rightarrow s \gamma$ transitions has been measured for the first time in b -baryon decays exploiting the decay chain $\Lambda_b^0 \rightarrow \Lambda \gamma$, $\Lambda \rightarrow p \pi^-$, which enables the determination of this observable from the angular distribution of the Λ decay products. The α_γ result is compatible with the SM prediction at the level of one standard deviation and provides new constraints that are compatible with previous measurements of the photon polarization in b -meson decays [7, 8]. Additionally, CP -breaking effects on this observable are studied for the first time and the results are compatible with CP symmetry. These results can be used to place constraints on the real and imaginary contributions of right-handed currents in BSM models. The precision of the results is dominated by the statistical uncertainty; furthermore, the dominant systematic uncertainty, due to the angular shape of the background, can be reduced with more data. Consequently, future data that will be collected by the LHCb experiment during the next decade will enable significant improvements of these results.

Acknowledgements

We express our gratitude to our colleagues in the CERN accelerator departments for the excellent performance of the LHC. We thank the technical and administrative staff at the LHCb institutes. We acknowledge support from CERN and from the national agencies: CAPES, CNPq, FAPERJ and FINEP (Brazil); MOST and NSFC (China); CNRS/IN2P3 (France); BMBF, DFG and MPG (Germany); INFN (Italy); NWO (Netherlands); MNiSW and NCN (Poland); MEN/IFA (Romania); MSHE (Russia); MICINN (Spain); SNSF and SER (Switzerland); NASU (Ukraine); STFC (United Kingdom); DOE NP and NSF (USA). We acknowledge the computing resources that are provided by CERN, IN2P3 (France), KIT and DESY (Germany), INFN (Italy), SURF (Netherlands), PIC (Spain), GridPP (United Kingdom), RRCKI and Yandex LLC (Russia), CSCS (Switzerland), IFIN-HH (Romania), CBPF (Brazil), PL-GRID (Poland) and NERSC (USA). We are indebted to the communities behind the multiple open-source software packages on which we depend. Individual groups or members have received support from ARC and ARDC (Australia); AvH Foundation (Germany); EPLANET, Marie Skłodowska-Curie Actions and ERC (European Union); A*MIDEX, ANR, IPhU and Labex P2IO, and Région Auvergne-Rhône-Alpes (France); Key Research Program of Frontier Sciences of CAS, CAS

PIFI, CAS CCEPP, Fundamental Research Funds for the Central Universities, and Sci. & Tech. Program of Guangzhou (China); RFBR, RSF and Yandex LLC (Russia); GVA, XuntaGal and GENCAT (Spain); the Leverhulme Trust, the Royal Society and UKRI (United Kingdom).

1 Supplemental material for PRL

The measurement of α_γ in this paper is used to place constraints on the electromagnetic dipole Wilson coefficients of the effective Hamiltonian of the $b \rightarrow s\gamma$ transition, namely $\mathcal{C}_7^{(\text{eff})}$ and $\mathcal{C}'_7^{(\text{eff})}$. The leading order expression of α_γ in terms of Wilson coefficients is used within the `flavio` package [36] to this end. This enables the experimental exclusion of two solutions with large real values of $\mathcal{C}_7^{(\text{eff})}$ and $\mathcal{C}'_7^{(\text{eff})}$ which, although phenomenologically unfavored, were experimentally allowed by all the previous measurements, as shown in Fig. 4 (top).

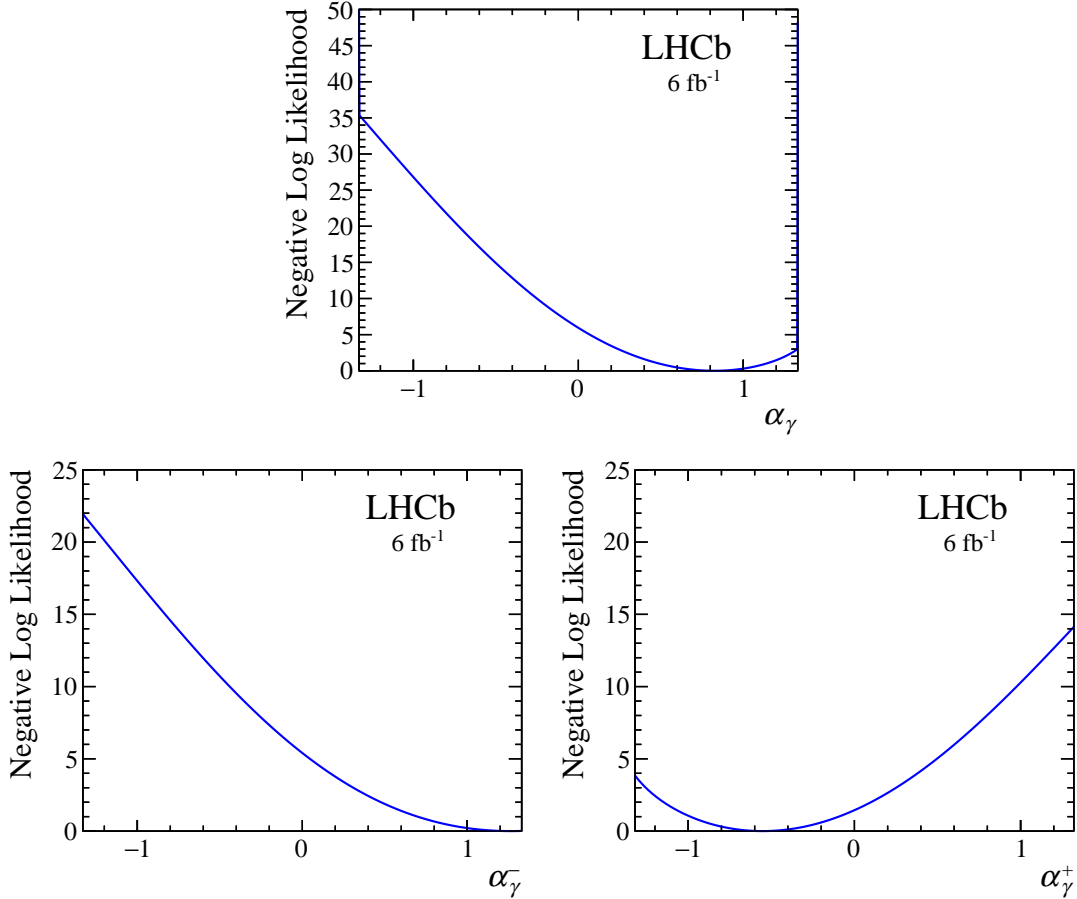


Figure 3: Profile of the negative log likelihood along the (top) combined, (bottom-left) $\Lambda_b^0 \rightarrow \Lambda\gamma$ and (bottom-right) $\bar{\Lambda}_b^0 \rightarrow \bar{\Lambda}\gamma$ photon polarization values (α_γ , α_γ^- and α_γ^+ , respectively).

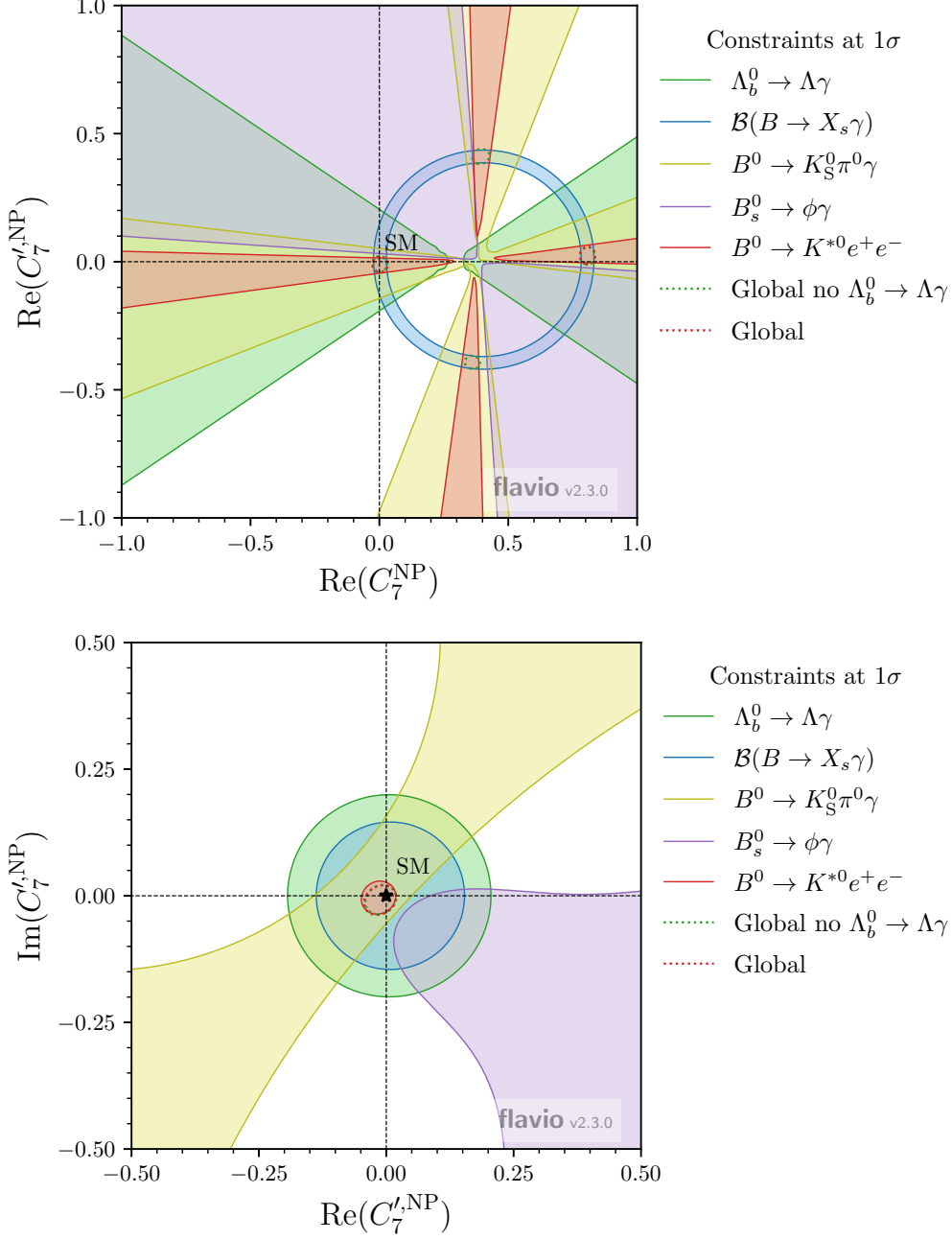


Figure 4: Constraints at the 1σ level on the new physics contributions to the (top) left- and right-handed Wilson coefficients, $C_7^{(\text{eff})}$ and $C_7'^{(\text{eff})}$ and on the (bottom) real and imaginary parts of $C_7'^{(\text{eff})}$. In the latter, the $C_7^{(\text{eff})}$ coefficient is fixed to its SM value. The measurements of the inclusive branching fraction, $\mathcal{B}(B \rightarrow X_s \gamma)$, and the $B^0 \rightarrow K_S^0 \pi^0 \gamma$ mixing-induced CP asymmetry by the Belle and BaBar experiments [5,6] are shown in blue and yellow, respectively, the $B_s^0 \rightarrow \phi \gamma$ and $B^0 \rightarrow K^{*0} e^+ e^-$ measurements by the LHCb experiment [7,8] in purple and red, respectively, and the α_γ measurement presented in this paper in green. The global fit is shown in dashed red (green) lines including (excluding) this measurement.

References

- [1] D. Atwood, M. Gronau, and A. Soni, *Mixing induced CP asymmetries in radiative B decays in and beyond the standard model*, Phys. Rev. Lett. **79** (1997) 185, arXiv:hep-ph/9704272.
- [2] G. Hiller and A. Kagan, *Probing for new physics in polarized Λ_b decays at the Z*, Phys. Rev. **D65** (2002) 074038, arXiv:hep-ph/0108074.
- [3] F. Legger and T. Schietinger, *Photon helicity in $\Lambda_b \rightarrow pK\gamma$ decays*, Phys. Lett. **B645** (2007) 204, Erratum ibid. **B647** (2007) 527, arXiv:hep-ph/0605245.
- [4] E. Kou, C.-D. Lü, and F.-S. Yu, *Photon Polarization in the $b \rightarrow s\gamma$ processes in the Left-Right Symmetric Model*, JHEP **12** (2013) 102, arXiv:1305.3173.
- [5] BaBar collaboration, B. Aubert *et al.*, *Measurement of Time-Dependent CP Asymmetry in $B^0 \rightarrow K_S^0\pi^0\gamma$ Decays*, Phys. Rev. **D78** (2008) 071102, arXiv:0807.3103.
- [6] Belle collaboration, Y. Ushiroda *et al.*, *Time-Dependent CP Asymmetries in $B^0 \rightarrow K_S^0\pi^0\gamma$ transitions*, Phys. Rev. **D74** (2006) 111104, arXiv:hep-ex/0608017.
- [7] LHCb collaboration, R. Aaij *et al.*, *Measurement of CP-violating and mixing-induced observables in $B_s^0 \rightarrow \phi\gamma$ decays*, Phys. Rev. Lett. **123** (2019) 081802, arXiv:1905.06284.
- [8] LHCb collaboration, R. Aaij *et al.*, *Strong constraints on the $b \rightarrow s\gamma$ photon polarisation from $B^0 \rightarrow K^{*0}e^+e^-$ decays*, JHEP **12** (2020) 081, arXiv:2010.06011.
- [9] M. Gremm, F. Krüger, and L. M. Sehgal, *Angular distribution and polarization of photons in the inclusive decay $\Lambda_b^0 \rightarrow X_s\gamma$* , Phys. Lett. **B355** (1995) 579, arXiv:hep-ph/9505354.
- [10] T. Mannel and S. Recksiegel, *Flavor changing neutral current decays of heavy baryons: The Case $\Lambda_b^0 \rightarrow \Lambda\gamma$* , J. Phys. **G24** (1998) 979, arXiv:hep-ph/9701399.
- [11] LHCb collaboration, R. Aaij *et al.*, *First observation of the radiative $\Lambda_b^0 \rightarrow \Lambda\gamma$ decay*, Phys. Rev. Lett. **123** (2019) 031801, arXiv:1904.06697.
- [12] L. M. García Martín *et al.*, *Radiative b-baryon decays to measure the photon and b-baryon polarization*, Eur. Phys. J. **C79** (2019) 634.
- [13] CMS collaboration, A. M. Sirunyan *et al.*, *Measurement of the Λ_b polarization and angular parameters in $\Lambda_b \rightarrow J/\psi \Lambda$ decays from pp collisions at $\sqrt{s} = 7$ and 8 TeV*, Phys. Rev. **D97** (2018) 072010, arXiv:1802.04867.
- [14] LHCb collaboration, R. Aaij *et al.*, *Measurement of the $\Lambda_b^0 \rightarrow J/\psi\Lambda$ angular distribution and the Λ polarisation in pp collisions*, JHEP **06** (2020) 110, arXiv:2004.10563.
- [15] LHCb collaboration, R. Aaij *et al.*, *Measurement of the ratio of branching fractions $\mathcal{B}(B^0 \rightarrow K^{*0}\gamma)/\mathcal{B}(B_s^0 \rightarrow \phi\gamma)$ and the direct CP asymmetry in $B^0 \rightarrow K^{*0}\gamma$* , Nucl. Phys. **B867** (2013) 1, arXiv:1209.0313.

- [16] LHCb collaboration, A. A. Alves Jr. *et al.*, *The LHCb detector at the LHC*, JINST **3** (2008) S08005.
- [17] LHCb collaboration, R. Aaij *et al.*, *LHCb detector performance*, Int. J. Mod. Phys. **A30** (2015) 1530022, [arXiv:1412.6352](#).
- [18] LHCb collaboration, R. Aaij *et al.*, *First experimental study of photon polarization in radiative B_s^0 decays*, Phys. Rev. Lett. **118** (2017) 021801, [arXiv:1609.02032](#).
- [19] LHCb collaboration, R. Aaij *et al.*, *Measurement of the ratio of branching fractions $\mathcal{B}(B^0 \rightarrow K^{*0}\gamma)/\mathcal{B}(B_s^0 \rightarrow \phi\gamma)$* , Phys. Rev. **D85** (2012) 112013, [arXiv:1202.6267](#).
- [20] R. Aaij *et al.*, *The LHCb trigger and its performance in 2011*, JINST **8** (2013) P04022, [arXiv:1211.3055](#).
- [21] T. Sjöstrand, S. Mrenna, and P. Skands, *A brief introduction to PYTHIA 8.1*, Comput. Phys. Commun. **178** (2008) 852, [arXiv:0710.3820](#); T. Sjöstrand, S. Mrenna, and P. Skands, *PYTHIA 6.4 physics and manual*, JHEP **05** (2006) 026, [arXiv:hep-ph/0603175](#).
- [22] I. Belyaev *et al.*, *Handling of the generation of primary events in Gauss, the LHCb simulation framework*, J. Phys. Conf. Ser. **331** (2011) 032047.
- [23] D. J. Lange, *The EvtGen particle decay simulation package*, Nucl. Instrum. Meth. **A462** (2001) 152.
- [24] N. Davidson, T. Przedzinski, and Z. Was, *PHOTOS interface in C++: Technical and physics documentation*, Comp. Phys. Comm. **199** (2016) 86, [arXiv:1011.0937](#).
- [25] Geant4 collaboration, J. Allison *et al.*, *Geant4 developments and applications*, IEEE Trans. Nucl. Sci. **53** (2006) 270; Geant4 collaboration, S. Agostinelli *et al.*, *Geant4: A simulation toolkit*, Nucl. Instrum. Meth. **A506** (2003) 250.
- [26] M. Clemencic *et al.*, *The LHCb simulation application, Gauss: Design, evolution and experience*, J. Phys. Conf. Ser. **331** (2011) 032023.
- [27] LHCb collaboration, R. Aaij *et al.*, *Observation of the suppressed decay $\Lambda_b^0 \rightarrow p\pi^-\mu^+\mu^-$* , JHEP **04** (2017) 029, [arXiv:1701.08705](#).
- [28] Particle Data Group, P. A. Zyla *et al.*, *Review of particle physics*, Prog. Theor. Exp. Phys. **2020** (2020) 083C01.
- [29] L. Breiman, J. H. Friedman, R. A. Olshen, and C. J. Stone, *Classification and regression trees*, Wadsworth international group, Belmont, California, USA, 1984.
- [30] T. Chen and C. Guestrin, *XGBoost: A scalable tree boosting system*, in *Proceedings of the 22nd ACM SIGKDD International Conference on Knowledge Discovery and Data Mining*, KDD '16, (New York, NY, USA), 785–794, ACM, 2016.
- [31] F. Pedregosa *et al.*, *Scikit-learn: Machine learning in Python*, J. Machine Learning Res. **12** (2011) 2825, [arXiv:1201.0490](#), and online at <http://scikit-learn.org/stable/>.

- [32] T. Skwarnicki, *A study of the radiative cascade transitions between the Upsilon-prime and Upsilon resonances*, PhD thesis, Institute of Nuclear Physics, Krakow, 1986, DESY-F31-86-02.
- [33] G. J. Feldman and R. D. Cousins, *Unified approach to the classical statistical analysis of small signals*, Phys. Rev. **D57** (1998) 3873.
- [34] BESIII collaboration, M. Ablikim *et al.*, *Polarization and Entanglement in Baryon-Antibaryon Pair Production in Electron-Positron Annihilation*, Nature Phys. **15** (2019) 631, [arXiv:1808.08917](#).
- [35] LHCb collaboration, R. Aaij *et al.*, *Observation of a $\Lambda_b^0 - \bar{\Lambda}_b^0$ production asymmetry in proton-proton collisions at $\sqrt{s} = 7$ and 8 TeV*, JHEP **10** (2021) 060, [arXiv:2107.09593](#).
- [36] D. M. Straub, *flavio: a Python package for flavour and precision phenomenology in the Standard Model and beyond*, [arXiv:1810.08132](#).

LHCb collaboration

R. Aaij³², A.S.W. Abdelmotteleb⁵⁶, C. Abellán Beteta⁵⁰, F. Abudinén⁵⁶, T. Ackernley⁶⁰, B. Adeva⁴⁶, M. Adinolfi⁵⁴, H. Afsharnia⁹, C. Agapopoulou¹³, C.A. Aidala⁸⁷, S. Aiola²⁵, Z. Ajaltouni⁹, S. Akar⁶⁵, J. Albrecht¹⁵, F. Alessio⁴⁸, M. Alexander⁵⁹, A. Alfonso Alberio⁴⁵, Z. Aliouche⁶², G. Alkhazov³⁸, P. Alvarez Cartelle⁵⁵, S. Amato², J.L. Amey⁵⁴, Y. Amhis¹¹, L. An⁴⁸, L. Anderlini²², A. Andreianov³⁸, M. Andreotti²¹, F. Archilli¹⁷, A. Artamonov⁴⁴, M. Artuso⁶⁸, K. Arzymatov⁴², E. Aslanides¹⁰, M. Atzeni⁵⁰, B. Audurier¹², S. Bachmann¹⁷, M. Bachmayer⁴⁹, J.J. Back⁵⁶, P. Baladron Rodriguez⁴⁶, V. Balagura¹², W. Baldini²¹, J. Baptista Leite¹, M. Barbetti²², R.J. Barlow⁶², S. Barsuk¹¹, W. Barter⁶¹, M. Bartolini^{24,h}, F. Baryshnikov⁸³, J.M. Basels¹⁴, S. Bashir³⁴, G. Bassi²⁹, B. Batsukh⁶⁸, A. Battig¹⁵, A. Bay⁴⁹, A. Beck⁵⁶, M. Becker¹⁵, F. Bedeschi²⁹, I. Bediaga¹, A. Beiter⁶⁸, V. Belavin⁴², S. Belin²⁷, V. Bellee⁵⁰, K. Belous⁴⁴, I. Belov⁴⁰, I. Belyaev⁴¹, G. Bencivenni²³, E. Ben-Haim¹³, A. Berezhnoy⁴⁰, R. Bernet⁵⁰, D. Berninghoff¹⁷, H.C. Bernstein⁶⁸, C. Bertella⁶², A. Bertolin²⁸, C. Betancourt⁵⁰, F. Betti⁴⁸, Ia. Bezshyiko⁵⁰, S. Bhasin⁵⁴, J. Bhom³⁵, L. Bian⁷³, M.S. Bieker¹⁵, S. Bifani⁵³, P. Billoir¹³, M. Birch⁶¹, F.C.R. Bishop⁵⁵, A. Bitadze⁶², A. Bizzeti^{22,k}, M. Bjørn⁶³, M.P. Blago⁴⁸, T. Blake⁵⁶, F. Blanc⁴⁹, S. Blusk⁶⁸, D. Bobulska⁵⁹, J.A. Boelhauve¹⁵, O. Boente Garcia⁴⁶, T. Boettcher⁶⁵, A. Boldyrev⁸², A. Bondar⁴³, N. Bondar^{38,48}, S. Borghi⁶², M. Borisyak⁴², M. Borsato¹⁷, J.T. Borsuk³⁵, S.A. Bouchiba⁴⁹, T.J.V. Bowcock⁶⁰, A. Boyer⁴⁸, C. Bozzi²¹, M.J. Bradley⁶¹, S. Braun⁶⁶, A. Brea Rodriguez⁴⁶, J. Brodzicka³⁵, A. Brossa Gonzalo⁵⁶, D. Brundu²⁷, A. Buonauro⁵⁰, L. Buonincontri²⁸, A.T. Burke⁶², C. Burr⁴⁸, A. Bursche⁷², A. Butkevich³⁹, J.S. Butter³², J. Buytaert⁴⁸, W. Byczynski⁴⁸, S. Cadeddu²⁷, H. Cai⁷³, R. Calabrese^{21,f}, L. Calefice^{15,13}, L. Calero Diaz²³, S. Cali²³, R. Calladine⁵³, M. Calvi^{26,j}, M. Calvo Gomez⁸⁵, P. Camargo Magalhaes⁵⁴, P. Campana²³, A.F. Campoverde Quezada⁶, S. Capelli^{26,j}, L. Capriotti^{20,d}, A. Carbone^{20,d}, G. Carboni³¹, R. Cardinale^{24,h}, A. Cardini²⁷, I. Carli⁴, P. Carniti^{26,j}, L. Carus¹⁴, K. Carvalho Akiba³², A. Casais Vidal⁴⁶, G. Casse⁶⁰, M. Cattaneo⁴⁸, G. Cavallero⁴⁸, S. Celani⁴⁹, J. Cerasoli¹⁰, D. Cervenkov⁶³, A.J. Chadwick⁶⁰, M.G. Chapman⁵⁴, M. Charles¹³, Ph. Charpentier⁴⁸, G. Chatzikonstantinidis⁵³, C.A. Chavez Barajas⁶⁰, M. Chefdeville⁸, C. Chen³, S. Chen⁴, A. Chernov³⁵, V. Chobanova⁴⁶, S. Cholak⁴⁹, M. Chruszcz³⁵, A. Chubykin³⁸, V. Chulikov³⁸, P. Ciambrone²³, M.F. Cicala⁵⁶, X. Cid Vidal⁴⁶, G. Ciezarek⁴⁸, P.E.L. Clarke⁵⁸, M. Clemencic⁴⁸, H.V. Cliff⁵⁵, J. Closier⁴⁸, J.L. Cobbledick⁶², V. Coco⁴⁸, J.A.B. Coelho¹¹, J. Cogan¹⁰, E. Cogneras⁹, L. Cojocariu³⁷, P. Collins⁴⁸, T. Colombo⁴⁸, L. Congedo^{19,c}, A. Contu²⁷, N. Cooke⁵³, G. Coombs⁵⁹, I. Corredoira⁴⁶, G. Corti⁴⁸, C.M. Costa Sobral⁵⁶, B. Couturier⁴⁸, D.C. Craik⁶⁴, J. Crkovská⁶⁷, M. Cruz Torres¹, R. Currie⁵⁸, C.L. Da Silva⁶⁷, S. Dadabaev⁸³, L. Dai⁷¹, E. Dall'Occo¹⁵, J. Dalseno⁴⁶, C. D'Ambrosio⁴⁸, A. Danilina⁴¹, P. d'Argent⁴⁸, J.E. Davies⁶², A. Davis⁶², O. De Aguiar Francisco⁶², K. De Bruyn⁷⁹, S. De Capua⁶², M. De Cian⁴⁹, J.M. De Miranda¹, L. De Paula², M. De Serio^{19,c}, D. De Simone⁵⁰, P. De Simone²³, F. De Vellis¹⁵, J.A. de Vries⁸⁰, C.T. Dean⁶⁷, F. Debernardis^{19,c}, D. Decamp⁸, V. Dedu¹⁰, L. Del Buono¹³, B. Delaney⁵⁵, H.-P. Dembinski¹⁵, A. Dendek³⁴, V. Denysenko⁵⁰, D. Derkach⁸², O. Deschamps⁹, F. Desse¹¹, F. Dettori^{27,e}, B. Dey⁷⁷, A. Di Cicco²³, P. Di Nezza²³, S. Didenko⁸³, L. Dieste Maronas⁴⁶, H. Dijkstra⁴⁸, V. Dobishuk⁵², C. Dong³, A.M. Donohoe¹⁸, F. Dordei²⁷, A.C. dos Reis¹, L. Douglas⁵⁹, A. Dovbnya⁵¹, A.G. Downes⁸, M.W. Dudek³⁵, L. Dufour⁴⁸, V. Duk⁷⁸, P. Durante⁴⁸, J.M. Durham⁶⁷, D. Dutta⁶², A. Dziurda³⁵, A. Dzyuba³⁸, S. Easo⁵⁷, U. Egede⁶⁹, V. Egorychev⁴¹, S. Eidelman^{43,u,†}, S. Eisenhardt⁵⁸, S. Ek-In⁴⁹, L. Eklund^{59,86}, S. Ely⁶⁸, A. Ene³⁷, E. Eppele⁶⁷, S. Escher¹⁴, J. Eschle⁵⁰, S. Esen¹³, T. Evans⁴⁸, A. Falabella²⁰, J. Fan³, Y. Fan⁶, B. Fang⁷³, S. Farry⁶⁰, D. Fazzini^{26,j}, M. Féo⁴⁸, A. Fernandez Prieto⁴⁶, A.D. Fernez⁶⁶, F. Ferrari^{20,d}, L. Ferreira Lopes⁴⁹, F. Ferreira Rodrigues², S. Ferreres Sole³², M. Ferrillo⁵⁰, M. Ferro-Luzzi⁴⁸, S. Filippov³⁹, R.A. Fini¹⁹, M. Fiorini^{21,f}, M. Firlej³⁴, K.M. Fischer⁶³, D.S. Fitzgerald⁸⁷,

C. Fitzpatrick⁶², T. Fiutowski³⁴, A. Fkiaras⁴⁸, F. Fleuret¹², M. Fontana¹³, F. Fontanelli^{24,h},
 R. Forty⁴⁸, D. Foulds-Holt⁵⁵, V. Franco Lima⁶⁰, M. Franco Sevilla⁶⁶, M. Frank⁴⁸, E. Franzoso²¹,
 G. Frau¹⁷, C. Frei⁴⁸, D.A. Friday⁵⁹, J. Fu⁶, Q. Fuehring¹⁵, E. Gabriel³², G. Galati^{19,c},
 A. Gallas Torreira⁴⁶, D. Galli^{20,d}, S. Gambetta^{58,48}, Y. Gan³, M. Gandelman², P. Gandini²⁵,
 Y. Gao⁵, M. Garau²⁷, L.M. Garcia Martin⁵⁶, P. Garcia Moreno⁴⁵, J. García Pardiñas^{26,j},
 B. Garcia Plana⁴⁶, F.A. Garcia Rosales¹², L. Garrido⁴⁵, C. Gaspar⁴⁸, R.E. Geertsema³²,
 D. Gerick¹⁷, L.L. Gerken¹⁵, E. Gersabeck⁶², M. Gersabeck⁶², T. Gershon⁵⁶, D. Gerstel¹⁰,
 L. Giambastiani²⁸, V. Gibson⁵⁵, H.K. Giemza³⁶, A.L. Gilman⁶³, M. Giovannetti^{23,p},
 A. Gioventù⁴⁶, P. Gironella Gironell⁴⁵, L. Giubega³⁷, C. Giugliano^{21,f,48}, K. Gizdov⁵⁸,
 E.L. Gkougkousis⁴⁸, V.V. Gligorov¹³, C. Göbel⁷⁰, E. Golobardes⁸⁵, D. Golubkov⁴¹,
 A. Golutvin^{61,83}, A. Gomes^{1,a}, S. Gomez Fernandez⁴⁵, F. Goncalves Abrantes⁶³, M. Goncerz³⁵,
 G. Gong³, P. Gorbounov⁴¹, I.V. Gorelov⁴⁰, C. Gotti²⁶, E. Govorkova⁴⁸, J.P. Grabowski¹⁷,
 T. Grammatico¹³, L.A. Granado Cardoso⁴⁸, E. Graugés⁴⁵, E. Graverini⁴⁹, G. Graziani²²,
 A. Grecu³⁷, L.M. Greeven³², N.A. Grieser⁴, L. Grillo⁶², S. Gromov⁸³, B.R. Gruberg Cazon⁶³,
 C. Gu³, M. Guarise²¹, M. Guittiere¹¹, P. A. Günther¹⁷, E. Gushchin³⁹, A. Guth¹⁴, Y. Guz⁴⁴,
 T. Gys⁴⁸, T. Hadavizadeh⁶⁹, G. Haefeli⁴⁹, C. Haen⁴⁸, J. Haimberger⁴⁸, T. Halewood-leagas⁶⁰,
 P.M. Hamilton⁶⁶, J.P. Hammerich⁶⁰, Q. Han⁷, X. Han¹⁷, T.H. Hancock⁶³, E.B. Hansen⁶²,
 S. Hansmann-Menzemer¹⁷, N. Harnew⁶³, T. Harrison⁶⁰, C. Hasse⁴⁸, M. Hatch⁴⁸, J. He^{6,b},
 M. Hecker⁶¹, K. Heijhoff³², K. Heinicke¹⁵, A.M. Hennequin⁴⁸, K. Hennessy⁶⁰, L. Henry⁴⁸,
 J. Heuel¹⁴, A. Hicheur², D. Hill⁴⁹, M. Hilton⁶², S.E. Hollitt¹⁵, R. Hou⁷, Y. Hou⁸, J. Hu¹⁷,
 J. Hu⁷², W. Hu⁷, X. Hu³, W. Huang⁶, X. Huang⁷³, W. Hulsbergen³², R.J. Hunter⁵⁶,
 M. Hushchyn⁸², D. Hutchcroft⁶⁰, D. Hynds³², P. Ibis¹⁵, M. Idzik³⁴, D. Ilin³⁸, P. Ilten⁶⁵,
 A. Inglessi³⁸, A. Ishteev⁸³, K. Ivshin³⁸, R. Jacobsson⁴⁸, H. Jage¹⁴, S. Jakobsen⁴⁸, E. Jans³²,
 B.K. Jashal⁴⁷, A. Jawahery⁶⁶, V. Jevtic¹⁵, F. Jiang³, M. John⁶³, D. Johnson⁴⁸, C.R. Jones⁵⁵,
 T.P. Jones⁵⁶, B. Jost⁴⁸, N. Jurik⁴⁸, S.H. Kalavan Kadavath³⁴, S. Kandybei⁵¹, Y. Kang³,
 M. Karacson⁴⁸, M. Karpov⁸², F. Keizer⁴⁸, D.M. Keller⁶⁸, M. Kenzie⁵⁶, T. Ketel³³, B. Khanji¹⁵,
 A. Kharisova⁸⁴, S. Kholodenko⁴⁴, T. Kirn¹⁴, V.S. Kirsebom⁴⁹, O. Kitouni⁶⁴, S. Klaver³²,
 N. Kleijne²⁹, K. Klimaszewski³⁶, M.R. Kmiec³⁶, S. Kolliiev⁵², A. Kondybayeva⁸³,
 A. Konoplyannikov⁴¹, P. Kopciwicz³⁴, R. Kopecna¹⁷, P. Koppenburg³², M. Korolev⁴⁰,
 I. Kostiuk^{32,52}, O. Kot⁵², S. Kotriakhova^{21,38}, P. Kravchenko³⁸, L. Kravchuk³⁹,
 R.D. Krawczyk⁴⁸, M. Kreps⁵⁶, F. Kress⁶¹, S. Kretschmar¹⁴, P. Krokovny^{43,u}, W. Krupa³⁴,
 W. Krzemien³⁶, M. Kucharczyk³⁵, V. Kudryavtsev^{43,u}, H.S. Kuindersma^{32,33}, G.J. Kunde⁶⁷,
 T. Kvaratskheliya⁴¹, D. Lacarrere⁴⁸, G. Lafferty⁶², A. Lai²⁷, A. Lampis²⁷, D. Lancierini⁵⁰,
 J.J. Lane⁶², R. Lane⁵⁴, G. Lanfranchi²³, C. Langenbruch¹⁴, J. Langer¹⁵, O. Lantwin⁸³,
 T. Latham⁵⁶, F. Lazzari^{29,q}, R. Le Gac¹⁰, S.H. Lee⁸⁷, R. Lefèvre⁹, A. Leflat⁴⁰, S. Legotin⁸³,
 O. Leroy¹⁰, T. Lesiak³⁵, B. Leverington¹⁷, H. Li⁷², P. Li¹⁷, S. Li⁷, Y. Li⁴, Y. Li⁴, Z. Li⁶⁸,
 X. Liang⁶⁸, T. Lin⁶¹, R. Lindner⁴⁸, V. Lisovskyi¹⁵, R. Litvinov²⁷, G. Liu⁷², H. Liu⁶, Q. Liu⁶,
 S. Liu⁴, A. Lobo Salvia⁴⁵, A. Loi²⁷, J. Lomba Castro⁴⁶, I. Longstaff⁵⁹, J.H. Lopes²,
 S. López Soliño⁴⁶, G.H. Lovell⁵⁵, Y. Lu⁴, C. Lucarelli²², D. Lucchesi^{28,l}, S. Luchuk³⁹,
 M. Lucio Martinez³², V. Lukashenko^{32,52}, Y. Luo³, A. Lupato⁶², E. Luppi^{21,f}, O. Lupton⁵⁶,
 A. Lusiani^{29,m}, X. Lyu⁶, L. Ma⁴, R. Ma⁶, S. Maccolini^{20,d}, F. Macheferri¹¹, F. Maciuc³⁷,
 V. Macko⁴⁹, P. Mackowiak¹⁵, S. Maddrell-Mander⁵⁴, O. Madejczyk³⁴, L.R. Madhan Mohan⁵⁴,
 O. Maev³⁸, A. Maevskiy⁸², D. Maisuzenko³⁸, M.W. Majewski³⁴, J.J. Malczewski³⁵, S. Malde⁶³,
 B. Malecki⁴⁸, A. Malinin⁸¹, T. Maltsev^{43,u}, H. Malygina¹⁷, G. Manca^{27,e}, G. Mancinelli¹⁰,
 D. Manuzzi^{20,d}, D. Marangotto^{25,i}, J. Maratas^{9,s}, J.F. Marchand⁸, U. Marconi²⁰, S. Mariani^{22,g},
 C. Marin Benito⁴⁸, M. Marinangeli⁴⁹, J. Marks¹⁷, A.M. Marshall⁵⁴, P.J. Marshall⁶⁰,
 G. Martelli⁷⁸, G. Martellotti³⁰, L. Martinazzoli^{48,j}, M. Martinelli^{26,j}, D. Martinez Santos⁴⁶,
 F. Martinez Vidal⁴⁷, A. Massafferri¹, M. Materok¹⁴, R. Matev⁴⁸, A. Mathad⁵⁰, V. Matiunin⁴¹,
 C. Matteuzzi²⁶, K.R. Mattioli⁸⁷, A. Mauri³², E. Maurice¹², J. Mauricio⁴⁵, M. Mazurek⁴⁸,
 M. McCann⁶¹, L. McConnell¹⁸, T.H. Mcgrath⁶², N.T. Mchugh⁵⁹, A. McNab⁶², R. McNulty¹⁸,

J.V. Mead⁶⁰, B. Meadows⁶⁵, G. Meier¹⁵, N. Meinert⁷⁶, D. Melnychuk³⁶, S. Meloni^{26,j},
 M. Merk^{32,80}, A. Merli^{25,i}, L. Meyer Garcia², M. Mikhasenko⁴⁸, D.A. Milanese⁷⁴, E. Millard⁵⁶,
 M. Milovanovic⁴⁸, M.-N. Minard⁸, A. Minotti^{26,j}, L. Minzoni^{21,f}, S.E. Mitchell⁵⁸, B. Mitreska⁶²,
 D.S. Mittel¹⁵, A. Mödden¹⁵, R.A. Mohammed⁶³, R.D. Moise⁶¹, S. Mokhnenko⁸²,
 T. Mombächer⁴⁶, I.A. Monroy⁷⁴, S. Monteil⁹, M. Morandin²⁸, G. Morello²³, M.J. Morello^{29,m},
 J. Moron³⁴, A.B. Morris⁷⁵, A.G. Morris⁵⁶, R. Mountain⁶⁸, H. Mu³, F. Muheim^{58,48},
 M. Mulder⁴⁸, D. Müller⁴⁸, K. Müller⁵⁰, C.H. Murphy⁶³, D. Murray⁶², P. Muzzetto^{27,48},
 P. Naik⁵⁴, T. Nakada⁴⁹, R. Nandakumar⁵⁷, T. Nanut⁴⁹, I. Nasteva², M. Needham⁵⁸, I. Neri²¹,
 N. Neri^{25,i}, S. Neubert⁷⁵, N. Neufeld⁴⁸, R. Newcombe⁶¹, E.M. Niel¹¹, S. Nieswand¹⁴,
 N. Nikitin⁴⁰, N.S. Nolte⁶⁴, C. Normand⁸, C. Nunez⁸⁷, A. Oblakowska-Mucha³⁴, V. Obraztsov⁴⁴,
 T. Oeser¹⁴, D.P. O'Hanlon⁵⁴, S. Okamura²¹, R. Oldeman^{27,e}, F. Oliva⁵⁸, M.E. Olivares⁶⁸,
 C.J.G. Onderwater⁷⁹, R.H. O'Neil⁵⁸, J.M. Otalora Goicochea², T. Ovsianikova⁴¹, P. Owen⁵⁰,
 A. Oyanguren⁴⁷, K.O. Padeken⁷⁵, B. Pagare⁵⁶, P.R. Pais⁴⁸, T. Pajero⁶³, A. Palano¹⁹,
 M. Palutan²³, Y. Pan⁶², G. Panshin⁸⁴, A. Papanestis⁵⁷, M. Pappagallo^{19,c}, L.L. Pappalardo^{21,f},
 C. Pappenheimer⁶⁵, W. Parker⁶⁶, C. Parkes⁶², B. Passalacqua²¹, G. Passaleva²², A. Pastore¹⁹,
 M. Patel⁶¹, C. Patrignani^{20,d}, C.J. Pawley⁸⁰, A. Pearce⁴⁸, A. Pellegrino³², M. Pepe Altarelli⁴⁸,
 S. Perazzini²⁰, D. Pereima⁴¹, A. Pereiro Castro⁴⁶, P. Perret⁹, M. Petric^{59,48}, K. Petridis⁵⁴,
 A. Petrolini^{24,h}, A. Petrov⁸¹, S. Petrucci⁵⁸, M. Petruzzo²⁵, T.T.H. Pham⁶⁸, A. Philippov⁴²,
 L. Pica^{29,m}, M. Piccini⁷⁸, B. Pietrzyk⁸, G. Pietrzyk⁴⁹, M. Pili⁶³, D. Pinci³⁰, F. Pisani⁴⁸,
 M. Pizzichemi^{26,48,j}, Resmi P.K¹⁰, V. Placinta³⁷, J. Plews⁵³, M. Plo Casasus⁴⁶, F. Polci¹³,
 M. Poli Lener²³, M. Poliakov⁶⁸, A. Poluektov¹⁰, N. Polukhina^{83,t}, I. Polyakov⁶⁸, E. Polcarpo²,
 S. Ponce⁴⁸, D. Popov^{6,48}, S. Popov⁴², S. Poslavskii⁴⁴, K. Prasanth³⁵, L. Promberger⁴⁸,
 C. Prouve⁴⁶, V. Pugatch⁵², V. Puill¹¹, H. Pullen⁶³, G. Punzi^{29,n}, H. Qi³, W. Qian⁶, J. Qin⁶,
 N. Qin³, R. Quagliani⁴⁹, B. Quintana⁸, N.V. Raab¹⁸, R.I. Rabadan Trejo⁶, B. Rachwal³⁴,
 J.H. Rademacker⁵⁴, M. Rama²⁹, M. Ramos Pernas⁵⁶, M.S. Rangel², F. Ratnikov^{42,82},
 G. Raven³³, M. Reboud⁸, F. Redi⁴⁹, F. Reiss⁶², C. Remon Alepuz⁴⁷, Z. Ren³, V. Renaudin⁶³,
 R. Ribatti²⁹, S. Ricciardi⁵⁷, K. Rinnert⁶⁰, P. Robbe¹¹, G. Robertson⁵⁸, A.B. Rodrigues⁴⁹,
 E. Rodrigues⁶⁰, J.A. Rodriguez Lopez⁷⁴, E.R.R. Rodriguez Rodriguez⁴⁶, A. Rollings⁶³,
 P. Roloff⁴⁸, V. Romanovskiy⁴⁴, M. Romero Lamas⁴⁶, A. Romero Vidal⁴⁶, J.D. Roth⁸⁷,
 M. Rotondo²³, M.S. Rudolph⁶⁸, T. Ruf⁴⁸, R.A. Ruiz Fernandez⁴⁶, J. Ruiz Vidal⁴⁷,
 A. Ryzhikov⁸², J. Ryzka³⁴, J.J. Saborido Silva⁴⁶, N. Sagidova³⁸, N. Sahoo⁵⁶, B. Saitta^{27,e},
 M. Salomoni⁴⁸, C. Sanchez Gras³², R. Santacesaria³⁰, C. Santamarina Rios⁴⁶, M. Santimaria²³,
 E. Santovetti^{31,p}, D. Saranin⁸³, G. Sarpis¹⁴, M. Sarpis⁷⁵, A. Sarti³⁰, C. Satriano^{30,o}, A. Satta³¹,
 M. Saur¹⁵, D. Savrina^{41,40}, H. Sazak⁹, L.G. Scantlebury Smead⁶³, A. Scarabotto¹³, S. Schael¹⁴,
 S. Scherl⁶⁰, M. Schiller⁵⁹, H. Schindler⁴⁸, M. Schmelling¹⁶, B. Schmidt⁴⁸, S. Schmitt¹⁴,
 O. Schneider⁴⁹, A. Schopper⁴⁸, M. Schubiger³², S. Schulte⁴⁹, M.H. Schune¹¹, R. Schwemmer⁴⁸,
 B. Sciascia^{23,48}, S. Sellam⁴⁶, A. Semennikov⁴¹, M. Senghi Soares³³, A. Sergi^{24,h}, N. Serra⁵⁰,
 L. Sestini²⁸, A. Seuthe¹⁵, Y. Shang⁵, D.M. Shangase⁸⁷, M. Shapkin⁴⁴, I. Shchemerov⁸³,
 L. Shchutka⁴⁹, T. Shears⁶⁰, L. Shekhtman^{43,u}, Z. Shen⁵, V. Shevchenko⁸¹, E.B. Shields^{26,j},
 Y. Shimizu¹¹, E. Shmanin⁸³, J.D. Shupperd⁶⁸, B.G. Siddi²¹, R. Silva Coutinho⁵⁰, G. Simi²⁸,
 S. Simone^{19,c}, N. Skidmore⁶², T. Skwarnicki⁶⁸, M.W. Slater⁵³, I. Slazyk^{21,f}, J.C. Smallwood⁶³,
 J.G. Smeaton⁵⁵, A. Smetkina⁴¹, E. Smith⁵⁰, M. Smith⁶¹, A. Snoch³², M. Soares²⁰,
 L. Soares Lavra⁹, M.D. Sokoloff⁶⁵, F.J.P. Soler⁵⁹, A. Solovev³⁸, I. Solovyev³⁸,
 F.L. Souza De Almeida², B. Souza De Paula², B. Spaan¹⁵, E. Spadaro Norella^{25,i}, P. Spradlin⁵⁹,
 F. Stagni⁴⁸, M. Stahl⁶⁵, S. Stahl⁴⁸, S. Stanislaus⁶³, O. Steinkamp^{50,83}, O. Stenyakin⁴⁴,
 H. Stevens¹⁵, S. Stone^{68,48}, M. Straticic³⁷, D. Strekalina⁸³, F. Suljik⁶³, J. Sun²⁷, L. Sun⁷³,
 Y. Sun⁶⁶, P. Sviha⁶², P.N. Swallow⁵³, K. Swientek³⁴, A. Szabelski³⁶, T. Szumlak³⁴,
 M. Szymanski⁴⁸, S. Taneja⁶², A.R. Tanner⁵⁴, M.D. Tat⁶³, A. Terentev⁸³, F. Teubert⁴⁸,
 E. Thomas⁴⁸, D.J.D. Thompson⁵³, K.A. Thomson⁶⁰, V. Tisserand⁹, S. T'Jampens⁸, M. Tobin⁴,
 L. Tomassetti^{21,f}, X. Tong⁵, D. Torres Machado¹, D.Y. Tou¹³, E. Trifonova⁸³, C. Trippl⁴⁹,

G. Tuci⁶, A. Tully⁴⁹, N. Tuning^{32,48}, A. Ukleja³⁶, D.J. Unverzagt¹⁷, E. Ursov⁸³, A. Usachov³², A. Ustyuzhanin^{42,82}, U. Uwer¹⁷, A. Vagner⁸⁴, V. Vagnoni²⁰, A. Valassi⁴⁸, G. Valenti²⁰, N. Valls Canudas⁸⁵, M. van Beuzekom³², M. Van Dijk⁴⁹, H. Van Hecke⁶⁷, E. van Herwijnen⁸³, C.B. Van Hulse¹⁸, M. van Veghel⁷⁹, R. Vazquez Gomez⁴⁵, P. Vazquez Regueiro⁴⁶, C. Vázquez Sierra⁴⁸, S. Vecchi²¹, J.J. Velthuis⁵⁴, M. Veltri^{22,r}, A. Venkateswaran⁶⁸, M. Veronesi³², M. Vesterinen⁵⁶, D. Vieira⁶⁵, M. Vieites Diaz⁴⁹, H. Viemann⁷⁶, X. Vilasis-Cardona⁸⁵, E. Vilella Figueras⁶⁰, A. Villa²⁰, P. Vincent¹³, F.C. Volle¹¹, D. Vom Bruch¹⁰, A. Vorobyev³⁸, V. Vorobyev^{43,u}, N. Voropaev³⁸, K. Vos⁸⁰, R. Waldi¹⁷, J. Walsh²⁹, C. Wang¹⁷, J. Wang⁵, J. Wang⁴, J. Wang³, J. Wang⁷³, M. Wang³, R. Wang⁵⁴, Y. Wang⁷, Z. Wang⁵⁰, Z. Wang³, Z. Wang⁶, J.A. Ward^{56,69}, N.K. Watson⁵³, S.G. Weber¹³, D. Websdale⁶¹, C. Weisser⁶⁴, B.D.C. Westhenry⁵⁴, D.J. White⁶², M. Whitehead⁵⁴, A.R. Wiederhold⁵⁶, D. Wiedner¹⁵, G. Wilkinson⁶³, M. Wilkinson⁶⁸, I. Williams⁵⁵, M. Williams⁶⁴, M.R.J. Williams⁵⁸, F.F. Wilson⁵⁷, W. Wislicki³⁶, M. Witek³⁵, L. Witola¹⁷, G. Wormser¹¹, S.A. Wotton⁵⁵, H. Wu⁶⁸, K. Wyllie⁴⁸, Z. Xiang⁶, D. Xiao⁷, Y. Xie⁷, A. Xu⁵, J. Xu⁶, L. Xu³, M. Xu⁷, Q. Xu⁶, Z. Xu⁵, Z. Xu⁶, D. Yang³, S. Yang⁶, Y. Yang⁶, Z. Yang⁵, Z. Yang⁶⁶, Y. Yao⁶⁸, L.E. Yeomans⁶⁰, H. Yin⁷, J. Yu⁷¹, X. Yuan⁶⁸, O. Yushchenko⁴⁴, E. Zaffaroni⁴⁹, M. Zavertyaev^{16,t}, M. Zdybal³⁵, O. Zenaiev⁴⁸, M. Zeng³, D. Zhang⁷, L. Zhang³, S. Zhang⁷¹, S. Zhang⁵, Y. Zhang⁵, Y. Zhang⁶³, A. Zharkova⁸³, A. Zhelezov¹⁷, Y. Zheng⁶, T. Zhou⁵, X. Zhou⁶, Y. Zhou⁶, V. Zhovkovska¹¹, X. Zhu³, X. Zhu⁷, Z. Zhu⁶, V. Zhukov^{14,40}, J.B. Zonneveld⁵⁸, Q. Zou⁴, S. Zucchelli^{20,d}, D. Zuliani²⁸, G. Zunica⁶².

¹Centro Brasileiro de Pesquisas Físicas (CBPF), Rio de Janeiro, Brazil

²Universidade Federal do Rio de Janeiro (UFRJ), Rio de Janeiro, Brazil

³Center for High Energy Physics, Tsinghua University, Beijing, China

⁴Institute Of High Energy Physics (IHEP), Beijing, China

⁵School of Physics State Key Laboratory of Nuclear Physics and Technology, Peking University, Beijing, China

⁶University of Chinese Academy of Sciences, Beijing, China

⁷Institute of Particle Physics, Central China Normal University, Wuhan, Hubei, China

⁸Univ. Savoie Mont Blanc, CNRS, IN2P3-LAPP, Annecy, France

⁹Université Clermont Auvergne, CNRS/IN2P3, LPC, Clermont-Ferrand, France

¹⁰Aix Marseille Univ, CNRS/IN2P3, CPPM, Marseille, France

¹¹Université Paris-Saclay, CNRS/IN2P3, IJCLab, Orsay, France

¹²Laboratoire Leprince-Ringuet, CNRS/IN2P3, Ecole Polytechnique, Institut Polytechnique de Paris, Palaiseau, France

¹³LPNHE, Sorbonne Université, Paris Diderot Sorbonne Paris Cité, CNRS/IN2P3, Paris, France

¹⁴I. Physikalisches Institut, RWTH Aachen University, Aachen, Germany

¹⁵Fakultät Physik, Technische Universität Dortmund, Dortmund, Germany

¹⁶Max-Planck-Institut für Kernphysik (MPIK), Heidelberg, Germany

¹⁷Physikalisches Institut, Ruprecht-Karls-Universität Heidelberg, Heidelberg, Germany

¹⁸School of Physics, University College Dublin, Dublin, Ireland

¹⁹INFN Sezione di Bari, Bari, Italy

²⁰INFN Sezione di Bologna, Bologna, Italy

²¹INFN Sezione di Ferrara, Ferrara, Italy

²²INFN Sezione di Firenze, Firenze, Italy

²³INFN Laboratori Nazionali di Frascati, Frascati, Italy

²⁴INFN Sezione di Genova, Genova, Italy

²⁵INFN Sezione di Milano, Milano, Italy

²⁶INFN Sezione di Milano-Bicocca, Milano, Italy

²⁷INFN Sezione di Cagliari, Monserrato, Italy

²⁸Università degli Studi di Padova, Università e INFN, Padova, Padova, Italy

²⁹INFN Sezione di Pisa, Pisa, Italy

³⁰INFN Sezione di Roma La Sapienza, Roma, Italy

³¹INFN Sezione di Roma Tor Vergata, Roma, Italy

- ³² *Nikhef National Institute for Subatomic Physics, Amsterdam, Netherlands*
- ³³ *Nikhef National Institute for Subatomic Physics and VU University Amsterdam, Amsterdam, Netherlands*
- ³⁴ *AGH - University of Science and Technology, Faculty of Physics and Applied Computer Science, Kraków, Poland*
- ³⁵ *Henryk Niewodniczanski Institute of Nuclear Physics Polish Academy of Sciences, Kraków, Poland*
- ³⁶ *National Center for Nuclear Research (NCBJ), Warsaw, Poland*
- ³⁷ *Horia Hulubei National Institute of Physics and Nuclear Engineering, Bucharest-Magurele, Romania*
- ³⁸ *Petersburg Nuclear Physics Institute NRC Kurchatov Institute (PNPI NRC KI), Gatchina, Russia*
- ³⁹ *Institute for Nuclear Research of the Russian Academy of Sciences (INR RAS), Moscow, Russia*
- ⁴⁰ *Institute of Nuclear Physics, Moscow State University (SINP MSU), Moscow, Russia*
- ⁴¹ *Institute of Theoretical and Experimental Physics NRC Kurchatov Institute (ITEP NRC KI), Moscow, Russia*
- ⁴² *Yandex School of Data Analysis, Moscow, Russia*
- ⁴³ *Budker Institute of Nuclear Physics (SB RAS), Novosibirsk, Russia*
- ⁴⁴ *Institute for High Energy Physics NRC Kurchatov Institute (IHEP NRC KI), Protvino, Russia, Protvino, Russia*
- ⁴⁵ *ICCUB, Universitat de Barcelona, Barcelona, Spain*
- ⁴⁶ *Instituto Galego de Física de Altas Enerxías (IGFAE), Universidade de Santiago de Compostela, Santiago de Compostela, Spain*
- ⁴⁷ *Instituto de Física Corpuscular, Centro Mixto Universidad de Valencia - CSIC, Valencia, Spain*
- ⁴⁸ *European Organization for Nuclear Research (CERN), Geneva, Switzerland*
- ⁴⁹ *Institute of Physics, Ecole Polytechnique Fédérale de Lausanne (EPFL), Lausanne, Switzerland*
- ⁵⁰ *Physik-Institut, Universität Zürich, Zürich, Switzerland*
- ⁵¹ *NSC Kharkiv Institute of Physics and Technology (NSC KIPT), Kharkiv, Ukraine*
- ⁵² *Institute for Nuclear Research of the National Academy of Sciences (KINR), Kyiv, Ukraine*
- ⁵³ *University of Birmingham, Birmingham, United Kingdom*
- ⁵⁴ *H.H. Wills Physics Laboratory, University of Bristol, Bristol, United Kingdom*
- ⁵⁵ *Cavendish Laboratory, University of Cambridge, Cambridge, United Kingdom*
- ⁵⁶ *Department of Physics, University of Warwick, Coventry, United Kingdom*
- ⁵⁷ *STFC Rutherford Appleton Laboratory, Didcot, United Kingdom*
- ⁵⁸ *School of Physics and Astronomy, University of Edinburgh, Edinburgh, United Kingdom*
- ⁵⁹ *School of Physics and Astronomy, University of Glasgow, Glasgow, United Kingdom*
- ⁶⁰ *Oliver Lodge Laboratory, University of Liverpool, Liverpool, United Kingdom*
- ⁶¹ *Imperial College London, London, United Kingdom*
- ⁶² *Department of Physics and Astronomy, University of Manchester, Manchester, United Kingdom*
- ⁶³ *Department of Physics, University of Oxford, Oxford, United Kingdom*
- ⁶⁴ *Massachusetts Institute of Technology, Cambridge, MA, United States*
- ⁶⁵ *University of Cincinnati, Cincinnati, OH, United States*
- ⁶⁶ *University of Maryland, College Park, MD, United States*
- ⁶⁷ *Los Alamos National Laboratory (LANL), Los Alamos, United States*
- ⁶⁸ *Syracuse University, Syracuse, NY, United States*
- ⁶⁹ *School of Physics and Astronomy, Monash University, Melbourne, Australia, associated to ⁵⁶*
- ⁷⁰ *Pontifícia Universidade Católica do Rio de Janeiro (PUC-Rio), Rio de Janeiro, Brazil, associated to ²*
- ⁷¹ *Physics and Micro Electronic College, Hunan University, Changsha City, China, associated to ⁷*
- ⁷² *Guangdong Provincial Key Laboratory of Nuclear Science, Guangdong-Hong Kong Joint Laboratory of Quantum Matter, Institute of Quantum Matter, South China Normal University, Guangzhou, China, associated to ³*
- ⁷³ *School of Physics and Technology, Wuhan University, Wuhan, China, associated to ³*
- ⁷⁴ *Departamento de Física, Universidad Nacional de Colombia, Bogota, Colombia, associated to ¹³*
- ⁷⁵ *Universität Bonn - Helmholtz-Institut für Strahlen und Kernphysik, Bonn, Germany, associated to ¹⁷*
- ⁷⁶ *Institut für Physik, Universität Rostock, Rostock, Germany, associated to ¹⁷*
- ⁷⁷ *Eotvos Lorand University, Budapest, Hungary, associated to ⁴⁸*
- ⁷⁸ *INFN Sezione di Perugia, Perugia, Italy, associated to ²¹*
- ⁷⁹ *Van Swinderen Institute, University of Groningen, Groningen, Netherlands, associated to ³²*
- ⁸⁰ *Universiteit Maastricht, Maastricht, Netherlands, associated to ³²*

- ⁸¹ *National Research Centre Kurchatov Institute, Moscow, Russia, associated to* ⁴¹
⁸² *National Research University Higher School of Economics, Moscow, Russia, associated to* ⁴²
⁸³ *National University of Science and Technology “MISIS”, Moscow, Russia, associated to* ⁴¹
⁸⁴ *National Research Tomsk Polytechnic University, Tomsk, Russia, associated to* ⁴¹
⁸⁵ *DS4DS, La Salle, Universitat Ramon Llull, Barcelona, Spain, associated to* ⁴⁵
⁸⁶ *Department of Physics and Astronomy, Uppsala University, Uppsala, Sweden, associated to* ⁵⁹
⁸⁷ *University of Michigan, Ann Arbor, United States, associated to* ⁶⁸

^a *Universidade Federal do Triângulo Mineiro (UFMT), Uberaba-MG, Brazil*

^b *Hangzhou Institute for Advanced Study, UCAS, Hangzhou, China*

^c *Università di Bari, Bari, Italy*

^d *Università di Bologna, Bologna, Italy*

^e *Università di Cagliari, Cagliari, Italy*

^f *Università di Ferrara, Ferrara, Italy*

^g *Università di Firenze, Firenze, Italy*

^h *Università di Genova, Genova, Italy*

ⁱ *Università degli Studi di Milano, Milano, Italy*

^j *Università di Milano Bicocca, Milano, Italy*

^k *Università di Modena e Reggio Emilia, Modena, Italy*

^l *Università di Padova, Padova, Italy*

^m *Scuola Normale Superiore, Pisa, Italy*

ⁿ *Università di Pisa, Pisa, Italy*

^o *Università della Basilicata, Potenza, Italy*

^p *Università di Roma Tor Vergata, Roma, Italy*

^q *Università di Siena, Siena, Italy*

^r *Università di Urbino, Urbino, Italy*

^s *MSU - Iligan Institute of Technology (MSU-IIT), Iligan, Philippines*

^t *P.N. Lebedev Physical Institute, Russian Academy of Science (LPI RAS), Moscow, Russia*

^u *Novosibirsk State University, Novosibirsk, Russia*

[†] *Deceased*